

## COLLECTIVITY IN LIGHT NUCLEI AND THE GDR

A. MAJ, J. STYCZEŃ, M. KMIECIK, P. BEDNARCZYK\*, M. BREKIESZ,  
J. GRĘBOSZ, M. LACH, W. MĘCZYŃSKI, M. ZIĘBLIŃSKI AND K. ZUBER

*The Niewodniczański Institute of Nuclear Physics, PAN  
ul. Radzikowskiego 152, 31-342 Kraków, Poland  
E-mail: Adam.Maj@ifj.edu.pl*

A. BRACCO, F. CAMERA, G. BENZONI, S. LEONI,  
B. MILLION AND O. WIELAND

*Dipartimento di Fisica, Università di Milano and INFN Sez. Milano  
Via Celoria 16, 20133 Milano, Italy*

The results are presented from the experiments using the EUROBALL and RFD/HECTOR arrays, concerning various aspects of collectivity in light nuclei. A superdeformed band in  $^{42}\text{Ca}$  was found. A comparison of the GDR line shape data with the predictions of the thermal shape fluctuation model, based on the most recent rotating liquid drop LSD calculations, shows evidence for a Jacobi shape transition in hot, rapidly rotating  $^{46}\text{Ti}$  and strong Coriolis effects in the GDR strength function. The preferential feeding of the SD band in  $^{42}\text{Ca}$  by the GDR low energy component was observed

### 1. Introduction

The excited states in nuclei are traditionally interpreted either as the collective excitations (e.g. in models based on rotating liquid drop), or as many single-particle excitations (e.g. in shell models), or as the coupling of single-particle excitations to the collective modes. Moreover, collective oscillations as the Giant Dipole Resonance (GDR) were found in hot nuclei and satisfactory interpreted within the statistical decay models and shape fluctuation models.

The light nuclei, with mass ranging from  $A=30$  to  $A=70$ , open new horizons for studying the excited states in nuclei. On one hand, the number of nucleons is here large enough to align and to form high spins. Because

---

\*Present address: GSI Darmstadt, Germany

of, however, the relatively light mass and consequently small value of the moment of inertia, the angular velocities associated with high spins are extremely large. One would, therefore, expect to observe much easier effects which are related to the rapid rotation, e.g. change in deformation, Coriolis effects, etc. On the other hand, the number of nucleons is small enough so that the band termination is easily reached, and the related single-particle effects are expected to prevail at highest spins. Also the shape fluctuations with such low number of nucleons are predicted to be sizeable. All this means that in light nuclei one should not expect to have clearly separated collective and single particle excitation modes, but rather a strong mixture of those two extreme approaches

## 2. Low-T regime: superdeformation in light nuclei

A textbook manifestation of the collective rotation in nuclei is the observation of the superdeformed (SD) bands. Such bands are characterized by a long cascade of  $\gamma$ -transitions, following the pattern of a rotor with constant moment of inertia, and with a value reflecting the 2:1 axis ratio of the nucleus. In light nuclei, the superdeformation is additionally associated with the extremely rapid rotation. Rotational frequency deduced for the SD bands known in this region can reach even 2 MeV. A typical example of the SD band in such nuclei is the one observed<sup>1</sup> in  $^{40}\text{Ca}$ . The kinematical moment of inertia of that SD band (shown in Fig. 1 with open circles) is constant as a function of rotational frequency, which proves a very stable superdeformed configuration. Similar SD bands were observed in several other nuclei in this mass region. Some of those bands, however, display less constant behavior in function of the rotational frequency. For example<sup>2</sup> in  $^{61}\text{Cu}$ , the SD band shows gradual decrease of the moment of inertia as a function of rotational frequency (Fig. 1, full diamonds). This may indicate an important contribution of non collective degrees of freedom in building states with high angular momentum when the band termination<sup>3</sup> is approached.

The main experimental difficulty in studying the high spin phenomena in the light mass region is an excessive Doppler broadening of lines in in-beam  $\gamma$ -spectra. This is due to a high recoil velocity of residues produced fusion-evaporation reactions and, of course, due to high energy of  $\gamma$ -rays expected to occur in light nuclei. This constrain can be minimized by making use of the Recoil Filter Detector (RFD)<sup>4</sup>, when coupled to the Ge-array. The RFD is a system of 18 heavy ion detectors distributed around the beam axis

placed downstream. It measures a time of flight of incoming residual nuclei produced in the reaction with respect to a beam pulse, as well as their flight direction. In this way the RFD enables a complete determination of the velocity vector of every recoiling nucleus, thus the event by event Doppler correction can be performed.

To study the high spin states in  $^{42}\text{Ca}$  nucleus in the experiment at VIVITRON accelerator of the IReS Laboratory of Strasbourg (France), the RFD was coupled to the EUROBALL. The resulting complex level scheme<sup>5</sup> was dominated by the single-particle excitation and by rotational bands of normal deformation. Nevertheless it was possible, due to the improved resolution, to single out a band showing the superdeformed character. The extracted moment of inertia of this band is plotted with full squares also in Fig. 1. It shows somewhat irregular behavior at low rotational frequencies, but at higher the behavior becomes smoother and the value of the relative kinematical moment of inertia is the same as for  $^{40}\text{Ca}$  and  $^{61}\text{Cu}$ . This band and other discrete transitions in this nucleus were used to analyze the properties of the GDR.

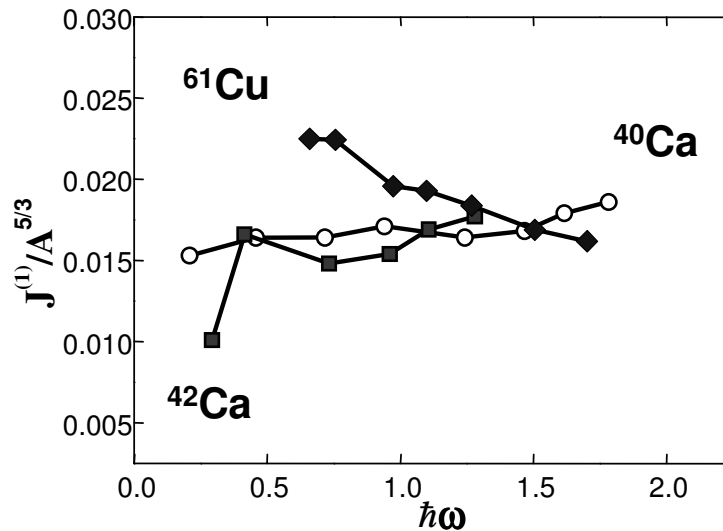


Figure 1. Relative kinematical moments of inertia for  $^{40}\text{Ca}$  (open circles),  $^{61}\text{Cu}$  (full diamonds) and  $^{42}\text{Ca}$  (full squares) as a function of rotational frequency.

### 3. High-T regime: Jacobi shape transitions and Coriolis effects in the GDR in light nuclei

The Jacobi shape transition, an abrupt change of nuclear shape from an oblate ellipsoid non-collectively rotating around its symmetry axis to an elongated prolate or triaxial shape, rotating collectively around the shortest axis has been predicted to appear in many nuclei at angular momenta close to the fission limit. In particular, recently developed LSD (Lublin-Strasbourg Drop) model<sup>6,7</sup> has been used to calculate the Jacobi transition mechanism in <sup>46</sup>Ti nucleus. The results of these calculation<sup>8</sup> have shown, that the equilibrium shape of the nucleus (in this liquid drop approximation) is spherical at  $I=0$  and nearly spherical for  $I<10\hbar$ , becomes oblate at larger spin value and the size of the oblate deformation becomes larger when the spin increases. At around  $I=28\hbar$  the Jacobi shape transition sets in: the nucleus becomes unstable towards triaxial and then (for  $I>34\hbar$ ) it follows prolate shape configurations, with rapidly increasing size of the deformation up to the fission limit (around  $I=40\hbar$ ).

Following these prediction, an another experiment at the VIVITRON accelerator was performed, using the EUROBALL phase IV Ge-array coupled to the HECTOR array<sup>9</sup>. In this experiment the <sup>46</sup>Ti compound nucleus was populated in the <sup>18</sup>O+<sup>28</sup>Si reaction at  $E_B=105$  MeV (for details see Ref. 10).

The GDR spectrum, gated on known, well resolved low energy  $\gamma$ -ray transitions of <sup>42</sup>Ca what selects high angular momentum region of the decaying compound nucleus, is shown in Fig. 2 (left panel) together with the best fit Monte Carlo Cascade calculations. The quality of the fit can be judged more clearly by inspecting the right panel of Fig. 2, where the GDR line shape, i.e. the extracted absorption cross-section using the method described in e.g. Ref. 11, is shown. One feature of the obtained GDR line shape is a broad high-energy component centered at around 25 MeV. Much more pronounced, however, is a narrow low-energy component at 10.5 MeV. This fit shows also that the average GDR line shape has to be approximated with at least 3 components.

In order to interpret this GDR line shape, we use the same approach as has been adopted in many studies concerning the GDR in hot and rotating nuclei (see e.g. Ref. 9), namely the thermal shape fluctuation model (see Ref. 12 and references therein) which assumes that the average GDR line shape is the weighted sum of individual (i.e. at given deformation) GDR line shapes. The weighting factors (the probability of finding the

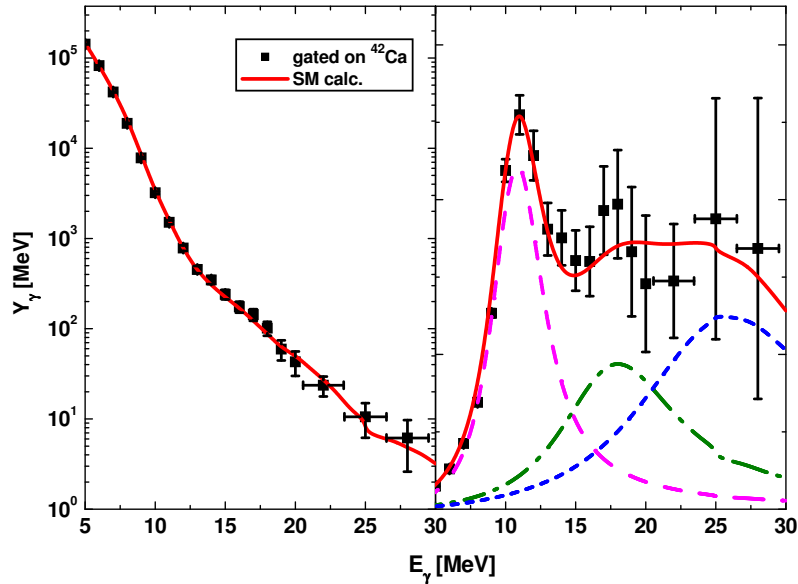


Figure 2. Left panel: The high-energy  $\gamma$ -ray spectrum gated by the  $^{42}\text{Ca}$  transitions and by high fold region, in comparison with the best fitting statistical model calculations (full drawn line) assuming a 3-Lorentzian GDR line shape. Right panel: The deduced experimental GDR strength function (full drawn line) together with best fitting 3-Lorentzian function and its individual components.

nucleus at a given deformation value) are calculated by using the macroscopic deformation-dependent LSD energies. In the calculations, we include the possibility of Coriolis splitting of the GDR strength function for given spin and deformation value using the rotating harmonic oscillator model<sup>13</sup>. Thus, for each deformation point the GDR line shape consists in general of 5-Lorentzian parametrization. The results for spin region  $I=28-34$  are presented together with the experimental GDR strength function in Fig. 3a.

A noteworthy good agreement between the theoretical predictions and the present experimental results can be observed. For comparison, the calculated averaged GDR line shape for  $I=24$ , i.e. in the oblate regime, is shown with dashed line in the same figure. This agreement might be an evidence of observation of the predicted Jacobi shape transition. Additional signature for the Jacobi transition may come from the presence of two other broad components in the strength function at higher energies both in the experiment and calculations. One component, at around 17 MeV, is clearly seen in the present data, and the other which is very broad (20-30 MeV)

can also be identified

To demonstrate the importance of the Coriolis effect, Fig. 3b shows the same calculations of the average GDR line shape when neglecting the Coriolis splitting. As can be seen, in this case the low-energy component has higher energy than the experimental one, and also the entire GDR line shape does not reproduce the experimental data. The predictions for the oblate regime ( $I=24$ ) are very weakly sensitive to the Coriolis effect.

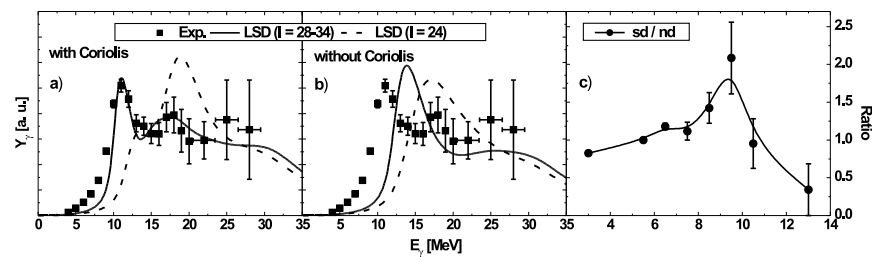


Figure 3. a) The full drawn line shows the theoretical prediction for the spin region 28-34 of the GDR line shape in  $^{46}\text{Ti}$  obtained from the thermal shape fluctuation model (including the Coriolis splitting of the GDR components) based on free energies from the LSD model calculations. The dashed line shows similar prediction for  $I=24$ . The filled squares are the experimental GDR strength function; b) The same, as in a), but in the calculations the Coriolis splitting was not taken into account; c) The ratio of the  $\gamma$ -ray intensity in the superdeformed band to the intensity in the normal deformed band in  $^{42}\text{Ca}$ , as a function of a gate set on the high energy  $\gamma$ -rays from the GDR decay of  $^{46}\text{Ti}$ .

#### 4. Link between high-T and low-T regimes: GDR feeding of the SD band in $^{42}\text{Ca}$

To see how the different regions of high-energy  $\gamma$ -rays feed the discrete lines in  $^{42}\text{Ca}$  residual nucleus, the gates (1 MeV wide) were set on the GDR spectrum and with such a condition the discrete line intensities were analyzed. The ratio of the intensity within the SD band in  $^{42}\text{Ca}$  (the one shown with full squares in Fig. 1) to the intensity of transition between states with normal deformation, is plotted in Fig. 3c. The ratio was normalized arbitrarily to 1 at 6 MeV. As can be seen, in the region 8-10 MeV the ratio is larger by a factor of 2 as compared to the low energy (statistical) region, and by factor almost 4 as compared to the normal GDR region ( $>12$  MeV). Considering that the gates were set on the raw spectrum (left panel of Fig. 2), not corrected for the detector's response function, this 8-10 MeV bump in

the ratio corresponds to the 10.5 MeV low energy component of the GDR strength function shown in Fig. 3a.

This might indicate that the low energy component of the GDR in the compound nucleus  $^{46}\text{Ti}$  feeds preferentially the SD band in the  $^{42}\text{Ca}$  evaporation residue. One can also speculate that the highly deformed shapes created by the Jacobi shape transition at rapidly spinning *hot* light nuclei persist the evaporation process and this results in population the superdeformed bands in *cold* high-spin residua.

One should note that similar preferential feeding of the SD-bands by the low energy component of the GDR has been observed<sup>14</sup> in the case of  $^{143}\text{Eu}$ .

## 5. Summary

A collective rotation forming the superdeformed band has been observed in  $^{42}\text{Ca}$ , with a moment of inertia similar to the other measured in this mass region. High-energy  $\gamma$ -ray spectrum from the hot  $^{46}\text{Ti}$  compound nucleus measured in coincidence with discrete transition in the  $^{42}\text{Ca}$  residues shows highly fragmented GDR strength function with a broad 15-25 MeV structure and a narrow low energy 10.5 MeV component. This can be interpreted as the result of Jacobi shape transition and strong Coriolis effects. In addition the low energy GDR component seems to feed preferentially the superdeformed band in  $^{42}\text{Ca}$ . This suggests that the very deformed shapes after the Jacobi shape transition in hot compound nucleus persist during the evaporation process. Thus the Jacobi shape transition in the compound nucleus might constitute kind of a gateway to very elongated, rapidly rotating cold nuclear shapes.

## Acknowledgments

We appreciate very much the help of B. Herskind from NBI Copenhagen; E. Farnea, G. de Angelis and D. Napoli from LNL Legnaro; S. Brambilla, M. Pignanelli and N. Blasi from Milano; M. Kicińska-Habior from Warsaw; J. Nyberg from Uppsala; C.M. Petrache from Camerino; D. Curien, J. Dudek and N. Dubray from Strasbourg and K. Pomorski from Lublin. A financial support from the Polish State Committee for Scientific Research (KBN Grant No. 2 P03B 118 22), the European Commission contract EUROVIV and the Italian INFN is acknowledged.

## References

1. E. Ideguchi, D.G. Sarantites, W. Reviol, A.V. Afanasjev, M. Devlin, C. Baktash, R.V.F. Janssens, D. Rudolph, A. Axelsson, M.P. Carpenter, A. Galindo-Uribarri, D.R. LaFosse, T. Lauritsen, F. Lerma, C.J. Lister, P. Reiter, D. Seweryniak, M. Weiszflog, and J.N. Wilson, *Phys. Rev. Lett.* **87**, 222501 (2001).
2. J. Dobaczewski, J.P. Vivien, K. Zuber, P. Bednarczyk, T. Byrski, D. Curien, G. de Angelis, O. Dorvaux, G. Duchene, E. Farnea, A. Gadea, B. Gall, J. Grębosz, R. Isocrate, A. Maj, W. Męczyński, J.C. Merdinger, A. Prevost, N. Redon, J. Robin, O. Stezowski, J. Styczeń, M. Ziębliński, *AIP Conf. Proc.* **701**, 273 (2004).
3. A.V. Afanasjev, I. Ragnarsson and P. Ring, *Phys. Rev.* **C59**, 3166 (1999).
4. P. Bednarczyk, W. Męczyński, J. Styczeń, J. Grębosz, M. Lach, A. Maj, M. Ziębliński, N. Kintz, J.C. Merdinger, N. Schulz, J.P. Vivien, A. Bracco, J.L. Pedroza, M.B. Smith, K.M. Spohr, *Acta Phys. Pol.* **B32**, 747 (2000).
5. M. Lach, J. Styczeń, W. Męczyński, P. Bednarczyk, A. Bracco, J. Grębosz, A. Maj, J.C. Merdinger, N. Schulz, M.B. Smith, K.M. Spohr, J.P. Vivien, and M. Ziębliński, *Eur Phys J.* **A12**, 381 (2001).
6. K. Pomorski and J. Dudek, *Phys. Rev.* **C67**, 044316 (2003).
7. J. Dudek, K. Pomorski, N. Schunck and N. Dubray, *Eur. Phys. J.* **A20**, 15 (2004).
8. A. Maj, M. Kmiecik, M. Brekiesz, J. Grębosz, W. Męczyński, J. Styczeń, M. Ziębliński, K. Zuber, A. Bracco, F. Camera, G. Benzoni, B. Million, N. Blasi, S. Brambilla, S. Leoni, M. Pignanelli, O. Wieland, B. Herskind, P. Bednarczyk, D. Curien, J.P. Vivien, E. Farnea, G. De Angelis, D.R. Napoli, J. Nyberg, M. Kicińska-Habior, C.M. Petrache, J. Dudek, and K. Pomorski, *Eur Phys J.* **A20**, 165 (2004).
9. A. Maj, J.J. Gaardhøje, A. Atac, S. Mitarai, J. Nyberg, A. Virtanen, A. Bracco, F. Camera, B. Million and M. Pignanelli, *Nucl. Phys.* **A571**, 185 (1994).
10. A. Maj, M. Kmiecik, A. Bracco, F. Camera, P. Bednarczyk, B. Herskind, S. Brambilla, G. Benzoni, M. Brekiesz, D. Curien, G. De Angelis, E. Farnea, J. Grębosz, M. Kicińska-Habior, S. Leoni, W. Męczyński, B. Million, D.R. Napoli, J. Nyberg, C.M. Petrache, J. Styczeń, O. Wieland, M. Ziębliński, K. Zuber, N. Dubray, J. Dudek and K. Pomorski, *Nucl. Phys.* **A731**, 319 (2004).
11. M. Kicińska-Habior, K.A. Snover, J.A. Behr, C.A. Gossett, Y. Alhassid and N. Whelan, *Phys. Lett.* **B308**, 225 (1993).
12. P.F. Bortignon, A. Bracco and R.A. Broglia, *Giant Resonances: Nuclear Structure at Finite Temperature*, Gordon Breach, New York, 1998.
13. K. Neergård, *Phys. Lett.* **B110**, 7 (1982).
14. G. Benzoni, A. Bracco, F. Camera, S. Leoni, B. Million, A. Maj, A. Algora, A. Axelsson, M. Bergstrom, N. Blasi, M. Castoldi, S. Frattini, A. Gadea, B. Herskind, M. Kmiecik, G. Lo Bianco, J. Nyberg, M. Pignanelli, J. Styczeń, O. Wieland, M. Ziębliński, A. Zucchiatti, *Phys. Lett.* **540B**, 199 (2002).